

The impact of seasonal changes in stratification on the dynamics of internal waves in the Sea of Okhotsk

Oxana E. Kurkina^a, Tatyana G. Talipova^{a,b}, Tarmo Soomere^{c,d}, Andrey A. Kurkin^a and Artem V. Rybin^a

^a Nizhny Novgorod State Technical University n.a. R.E. Alekseev, 603950 Nizhny Novgorod, Russia

^b Institute of Applied Physics, 603950 Nizhny Novgorod, Russia

^c Department of Cybernetics, School of Science, Tallinn University of Technology, 12618 Tallinn, Estonia; tarmo.soomere@cs.ioc.ee

^d Estonian Academy of Sciences, Kohtu 6, 10130 Tallinn, Estonia

Received 26 June 2017, accepted 7 August 2017, available online 28 November 2017

Abstract. The properties and dynamics of internal waves in the ocean crucially depend on the vertical structure of water masses. We present detailed analysis of the impact of spatial and seasonal variations in the density-driven stratification in the Sea of Okhotsk on the properties of the classic kinematic and nonlinear parameters of internal waves in this water body. The resulting maps of the phase speed of long internal waves and coefficients at various terms of the underlying Gardner's equation make it possible to rapidly determine the main properties of internal solitary waves in the region and to choose an adequate set of parameters of the relevant numerical models. It is shown that the phase speed of long internal waves almost does not depend on the particular season. The coefficient at the quadratic term of the underlying evolution equation is predominantly negative in summer and winter and therefore internal solitons usually have negative polarity. Numerical simulations of the formation of internal solitons and solibores indicate that seasonal variations in the coefficient at the cubic term of Gardner's equation lead to substantial variations in the shape of solibores.

Key words: internal waves, stratification, internal solitons, Gardner's equation, Sea of Okhotsk.

INTRODUCTION

Internal waves are an intrinsic constituent of dynamics of all stratified water bodies, having a particular role in the functioning of the entire ecosystem of seas and oceans. They provide massive transport of energy over large distances from their generation region to remote and partially sheltered areas under favourable conditions. Locally, they substantially contribute to the mixing of water masses and resuspension and transport of bottom sediment (Stastna & Lamb 2008; Reeder et al. 2011; Bourgault et al. 2014). In this way internal waves greatly impact the distribution of nutrients, often markedly relocate patches of plankton in the water column and thus play a crucial role in the formation of the biological productivity of seas and oceans (Vázquez et al. 2009; Pan et al. 2012).

The propagation and breaking of internal waves is often associated with the excitation of strong currents that serve as a major danger to deep-water engineering structures (Osborne 2010; Song et al. 2011; Stober &

Moum 2011). The presence of internal waves modifies the local field of water density and thus impacts the propagation regimes of acoustic waves through the water masses (Warn-Varnas et al. 2009; Rutenko 2010).

The main source of energy of internal waves in the open ocean and in most of shelf seas is the tidal motion. The parameters of internal waves generated, for example, via the interaction of a tidal wave and bathymetry substantially depend on the vertical structure of water density (local stratification) and the properties of currents in the wave generation and propagation area. While the field of currents often varies rapidly, changes in the stratification are usually slow but often extensive on a seasonal scale (Holloway et al. 1997). The intricacy of the entire phenomenon of internal waves and complexity of their generation and impact have initiated many studies into their dynamics. These studies are largely targeted to the understanding of this phenomenon in shelf seas that have large resources of oil and gas such as the South China Sea (Ramp et al. 2010; Liu et al. 2013; Alford et al. 2015; Xu et al. 2016).

© 2017 Authors. This is an Open Access article distributed under the terms and conditions of the Creative Commons Attribution 4.0 International Licence (<http://creativecommons.org/licenses/by/4.0>).

The options of analytical studies of internal waves are limited and the use of the relevant exact solutions for practical purposes is fairly complicated. For this reason the use of numerical simulations of different properties of internal waves (e.g., the evaluation of velocities of water parcels excited by the internal wave motion and associated impact on the underwater parts of engineering structures) is rapidly increasing (Kurkina & Talipova 2011; Si et al. 2012; Vlasenko & Stashchuk 2015; Kurkina et al. 2016). Such simulations of internal waves of the lowest mode often rely on the classic weakly nonlinear models of the family of Korteweg–de Vries equations. A natural extension of this family towards taking into account the impact of spatially inhomogeneous stratification patterns leads to so-called Gardner’s equation (Holloway et al. 1997; Grimshaw et al. 2004, 2010; Talipova et al. 2014, 2015).

The coefficients of this equation at a particular location depend on the properties of stratification in this location. A reliable implementation of models of this type thus requires an adequate representation of the horizontal variability in stratification along the wave propagation direction. The relevant information is commonly extracted either from in situ measurements or in a generalized form from contemporary hydrophysical data bases and atlases such as the *World Ocean Atlas* or *Generalized Digital Environmental Model*. These sources usually contain gridded monthly average vertical profiles of salinity and temperature, from which one can derive the required vertical density profiles. This approach has been used for the analysis of the properties of coefficients of Gardner’s equation and associated regimes of the propagation of internal waves in many regions of the World Ocean such as the Mediterranean Sea and the Black Sea (Ivanov et al. 1993; Kurkina et al. 2017a), several parts of the Arctic seas (Poloukhin et al. 2003; Polukhin et al. 2004), the Baltic Sea (Talipova et al. 1998; Kurkina et al. 2011) and the South China Sea (Grimshaw et al. 2010; Liao et al. 2014; Kurkina et al. 2017b).

The Sea of Okhotsk (Zonn & Kostianoy 2009) is a marginal sea on the eastern shelf of the Eurasian continent (Fig. 1). Its several features are similar to those of the Baltic Sea. It is separated from the western Pacific Ocean by the Kamchatka Peninsula in the east and by the chain of Kuril Islands in the southeast. The islands of Hokkaido and Sakhalin separate this water body from the Sea of Japan. Its area (1 583 000 km²) and mean depth (851 m) are much larger than the surface area and depth of the Baltic Sea. A voluminous discharge of the Amur River into the Sea of Okhotsk results in the rise of the freezing point of the sea and in this way supports the formation of the massive presence of ice floes during each winter.

In spite of severe climate and a location at comparatively high latitudes, the Sea of Okhotsk has a highly productive ecosystem and large fish stock. Extensive reserves of gas and oil below the seabed make this basin an attractive location for various engineering activities. The fastest development occurs in the nearshore of Sakhalin. While it is usually assumed that harsh ice conditions, frequent storm winds and severe seas create the greatest danger to the drilling rigs and other constructions in the Arctic region (Petterssen 2011), the situation in the Sea of Okhotsk is even more complicated because of the frequent presence of highly energetic internal waves. There exist only a few contact measurements of such structures in the shelf region of the Sea of Okhotsk. The existing records indicate that internal waves in this basin may have the appearance of internal solitons with an amplitude of 5–15 m and length of 200–400 m (Nagovitsyn & Pelinovsky 1988; Nagovitsyn et al. 1991). However, numerous signatures of single internal waves and various wave packets are evident in satellite photos (Jackson 2004) in many regions of the Sea of Okhotsk, including the above-mentioned nearshore of Sakhalin. Similarly to the situation in many other parts of the World Ocean, trains of internal waves have often a shape of localized wave packets whereas their leading waves are often the largest ones. As these trains frequently resemble combinations of internal solitary waves and undular bores, we shall call such trains solibores in what follows. The main source of energy of internal waves is the barotropic tide. Its motion gives rise to high-amplitude internal waves once in every 12.4 h. This feature leads to a highly periodic propagation pattern of internal waves in the Sea of Okhotsk.

In this paper we aim at the clarification of spatial distributions of the basic parameters that govern the propagation regime and the resulting seasonal variations in the main properties of internal waves in the Sea of Okhotsk. We employ a somewhat simplified approach in order to derive estimates of limiting values of internal wave properties. For this purpose it is to a first approximation acceptable to exclude the effect of the Earth’s rotation and to avoid the calculation of the exact location of the internal wave generation from internal tides.

These distributions reflect not only the geographic variability of the bathymetry and water masses of this basin but also mirror strong seasonal variations in the atmospheric and hydrographic features in the region. These parameters are crucial for both detailed simulations and express estimates of hydrodynamic loads to various engineering structures in the study area. The derived estimates are applied to evaluate the deviations of isopycnal surfaces from their undisturbed positions

under the impact of internal waves (equivalently, the amplitudes of internal waves) and velocity fields in such waves in prospective locations of oil and gas platforms on the shelf of Sakhalin.

The structure of the paper is as follows. We start from the construction of maps of seasonal variations in the basic parameters that characterize the stratification pattern of the water masses in the study area. This is followed by a short insight into the models commonly used for the description of long weakly nonlinear internal waves. Next, the maps of the core kinematic parameters and coefficients at nonlinear terms of the relevant Gardner's equation (often called nonlinear parameters) are presented. Finally, we provide a selection of results of the numerical simulation of properties of internal waves in winter and summer conditions and a short discussion of the main results.

SEASONAL VARIATIONS IN STRATIFICATION

The dynamics of the Sea of Okhotsk represent a combination of several common features of a coastal sea in some of its parts with the classic features of shelf seas in its deeper parts. While the average depth of that sea is 821 m, the largest depth reaches 3374 m in the Kuril (also Kuril–Kamchatka) trench. Its water masses interact with processes in the Pacific along many straits between different islands of the Greater Kuril Ridge and Lesser Kuril Ridge. Intense exchange of mass and energy with the Japan Sea occurs via the La Pérouse Strait (or Sōya Strait). Another connection to the Japan Sea exists via the Nevelskoy Strait, the Amur River estuary and Tartary Strait (or Gulf of Tartary).

The seabed of the Sea of Okhotsk represents three types of morphologic zones. Relatively shallow (depths >200 m) and wide (180–250 km) nearshore areas of the Asian continent and clearly narrower shallow nearshore zones of Sakhalin and the Kamchatka Peninsula cover about 20% of the entire sea and exhibit typical features of a shelf sea. The water depth increases more or less steadily along the continental slope from the nearshore towards the central Sea of Okhotsk where the water depth is between 1000 and 2000 m. This gently sloping domain covers about 65% of the Sea of Okhotsk. It contains several single underwater elevations and depressions with large gradients of the seabed and with typical horizontal and vertical scales of 10–20 km and 100–200 m, respectively. A deep-water trench, with depths exceeding 2500 m, represents about 8% of the sea surface.

The shelf sea in the vicinity of Sakhalin is located in the middle-latitude temperate climate zone where seasonal warming of surface waters substantially affects

the temporal course of the stratification of water masses. During winter months typically sea ice is formed on the surface. Ice cover is a standard feature in the nearshore of northern Sakhalin. The formation and melting of sea ice additionally contributes to the formation of and variation in the salinity-driven stratification. This impact often lasts until almost midsummer when sea ice finally melts.

Generalized and standardized information about the basic features of hydrophysical parameters of sea water and their seasonal variations has been integrated into the open source digital climatologic atlas *Generalized Digital Environment Model* (GDEM) (Teague et al. 1990). Its version 3.0 (Carnes 2009) provides monthly averaged coefficients of empirical formulas that represent the vertical profiles of temperature and salinity at 77 vertical levels. The information is gridded to a regular rectangular set with a horizontal resolution of $1/2^\circ$ in the open ocean. Many coastal areas and marginal seas have a resolution of this information of $1/6^\circ$.

The profiles have been calculated using the standard approach of Fofonoff & Millard (1983) based on the classic definition of the Brunt–Väisälä frequency $N(z)$:

$$N^2(z) = -\frac{g}{\rho_0(z)} \frac{d\rho_0(z)}{dz}. \quad (1)$$

Here z indicates the vertical location, g is acceleration due to gravity and $\rho_0(z)$ represents the vertical variation in water density.

The vertical structure of the Brunt–Väisälä frequency (and, consequently, the vertical structure of water masses) is greatly different in January and July (Fig. 2) on the continental shelf to the northeast of Sakhalin in an area where the density of existing observations is relatively high. Horizontal variations in the Brunt–Väisälä frequency and water density are relatively small and smooth for each of these months. The values of both quantities vary insignificantly between seasons in most of the water column and are almost constant below a depth of 250 m. All substantial changes in the water properties are concentrated in the uppermost layer with a thickness of 200–250 m. The variations in the Brunt–Väisälä frequency $N(z)$ are moderate in the entire water column along this profile in January (Fig. 2). The maximum values of this frequency reach 0.0065 s^{-1} during this month in both nearshore relatively shallow waters and in the deep part of the transect indicated in Fig. 1. The maximum values of $N(z)$ are much larger, up to 0.02 s^{-1} in July whereas these maxima are again almost constant along the transect.

Maps of spatial distributions of the maximum values N_{\max} of the Brunt–Väisälä frequency $N(z)$ (Fig. 3A, B) indicate that the vertical structure of water masses of the

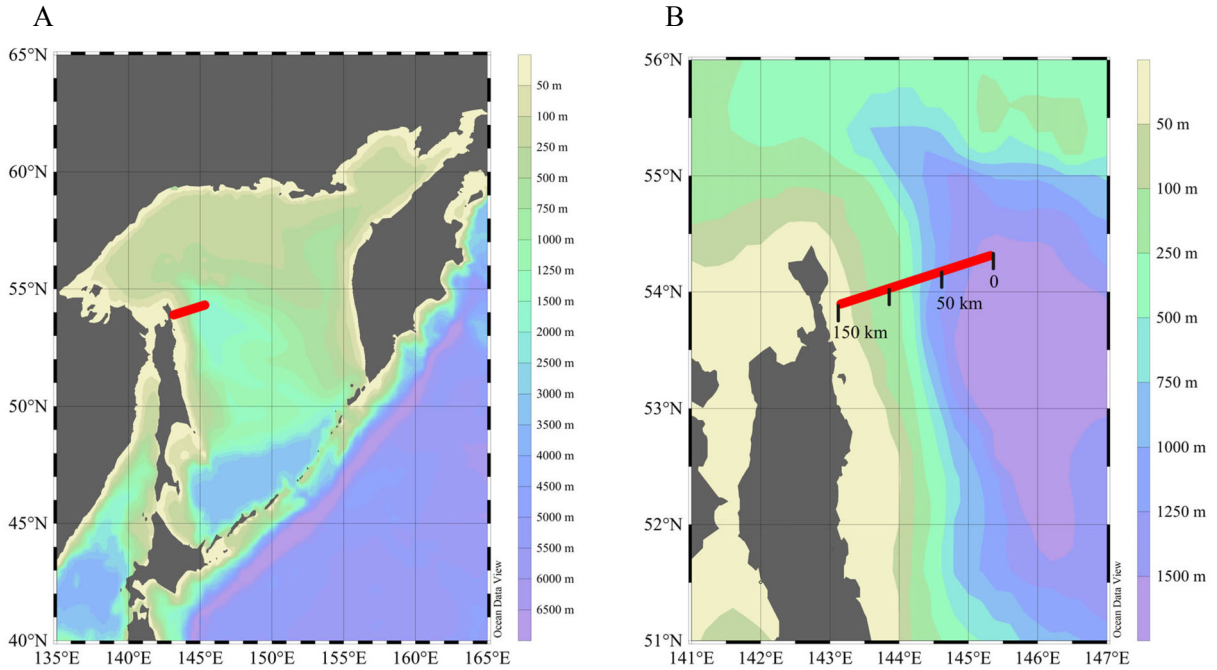


Fig. 1. Bathymetry of the Sea of Okhotsk (A) and its western section near Sakhalin (B). The red line near the northeastern coast of Sakhalin shows the location of the cross section (called transect below) for data presented in Fig. 2 and for the modelling of the transformation of the baroclinic internal tide into a solibore.

Sea of Okhotsk exhibits great seasonal variations. The maxima of N_{\max} in summer are, on average, four times as large as the relevant maxima in winter. This contrast is even larger near Magadan where N_{\max} in summer is up to six times as large as in winter. Figure 2 suggests that the variations in $N(z)$ are relatively small in winter. This assertion is confirmed by the narrowness of the empirical probability distribution of $N(z)$ (Fig. 3C). The relevant histogram indicates that the values of $N(z)$ are in the range of $0.002\text{--}0.01\text{ s}^{-1}$ and concentrated around the value of 0.005 s^{-1} . The similar distribution for July is much wider, contains the majority of values in the range of $0.01\text{--}0.038\text{ s}^{-1}$ and is centred at 0.025 s^{-1} .

The depth at which the maximum values N_{\max} of the Brunt–Väisälä frequency $N(z)$ occur (Fig. 4) strongly varies in both summer and winter. This depth is the smallest (10–20 m) in the deep part of the Sea of Okhotsk but much larger (40–60 m) on the northeastern shelf of Sakhalin and even greater on the northwestern shelf of this sea in January. The depth in question strongly decreases in summer. The maximum values N_{\max} are mostly observed in the surface layer at depths of 0–20 m. Only in a middle segment of the western shelf of Sakhalin the maximum values of $N(z)$ occur at depths of 30–35 m. The presented features suggest that propagation regimes of internal (solitary) waves may greatly vary depending on the particular season and geographical location.

KINEMATIC PARAMETERS OF LONG INTERNAL WAVES IN THE SEA OF OKHOTSK

A convenient model for the description of many properties of long internal waves of the first mode is the so-called extended Korteweg–de Vries equation with combined nonlinearity. This equation, often called Gardner’s equation, has been widely used for both theoretical and numerical studies of this phenomenon (Lamb & Yan 1996; Pelinovsky et al. 2007; Maderich et al. 2009, 2010; Talipova & Pelinovsky 2013; Talipova et al. 2014, 2015). This model equation has the following dimensional form:

$$\frac{\partial \eta}{\partial t} + (c + \alpha \eta + \alpha_1 \eta^2) \frac{\partial \eta}{\partial x} + \beta \frac{\partial^3 \eta}{\partial x^3} = 0, \quad (2)$$

where η denotes the deviation of the isopycnal surface from its undisturbed location (measured at a depth that corresponds to the maximum of the vertical mode), c is the phase speed of long internal waves, α is the coefficient at the quadratic term (often called the quadratic nonlinearity coefficient), α_1 is the coefficient at the cubic term (often called the cubic nonlinearity coefficient) and β is the coefficient at the linear (dispersive) term and is sometimes called the dispersion coefficient.

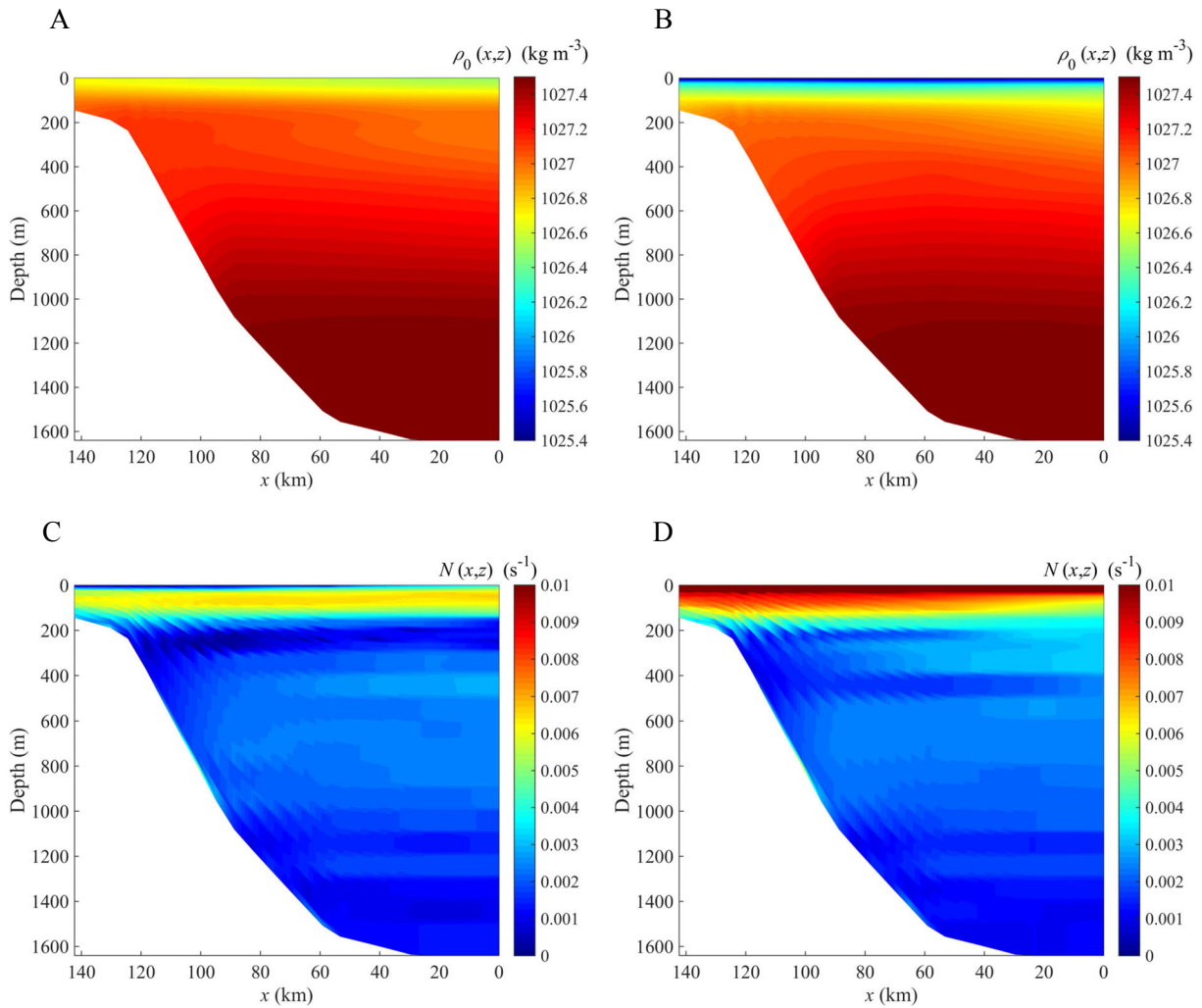


Fig. 2. Characteristic vertical structure of water density (A, B) and the Brunt–Väisälä frequency (C, D) in January (A, C) and July (B, D) along the cross section of the northeastern shelf of Sakhalin indicated in Fig. 1.

A description of the vertical structure and the phase speed of long linear internal waves c can be found (in the Boussinesq approximation) from the following Sturm–Liouville problem:

$$\frac{d^2\Phi}{dz^2} + \frac{N^2(z)}{c^2}\Phi = 0 \quad (3)$$

with homogeneous boundary conditions

$$\Phi(0) = \Phi(H) = 0. \quad (4)$$

Here Φ is so-called mode function that represents the vertical structure of internal waves, z is, as above, the vertical coordinate, $z = 0$ at the bottom, $z = H$ at the sea surface and the z -axis is directed upwards.

The theory of internal waves based on Gardner’s equation and Eqs (3), (4) is valid for any wave mode.

However, in practice this theory is usually applied to waves of the first or the second mode. The first mode corresponds to the case when the mode function $\Phi(z)$ does not vanish within the interval $[0, H]$ and the phase speed c is the largest eigenvalue of the Sturm–Liouville problem (3), (4). The second mode represents the case when $\Phi(z)$ has exactly one zero-crossing and two extreme values within the interval $[0, H]$. These cases cover more than 95% of all observations of internal waves in the World Ocean.

A unique solution for the Sturm–Liouville problem (3), (4) can be specified using certain additional conditions. It is customary to normalize the function $\Phi(z)$ for the waves of the first mode so that this function is positive and its maximum $\Phi_{\max}(z) = 1$. If this condition is applied, the function $\eta(x,t)$ describes deviations of the isopycnal surface from its undisturbed position at the location $z = z_{\max}$ where the maximum

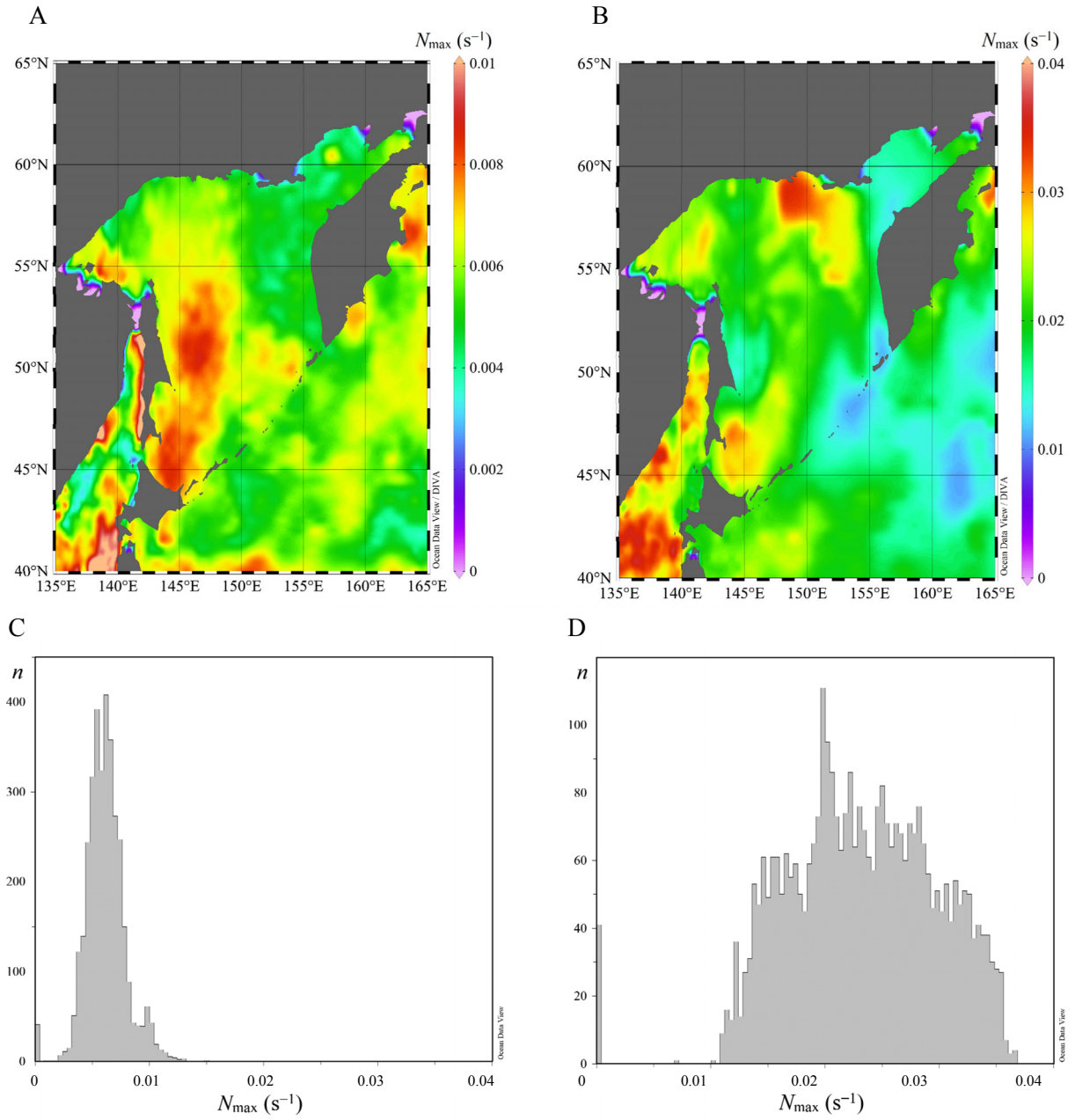


Fig. 3. Maps of maximum values N_{\max} of the Brunt–Väisälä frequency $N(z)$ (colour scale, s^{-1}) in January (**A**) and July (**B**) and histograms of the occurrence of different values of N_{\max} in January (**C**) and July (**D**). The entire range of values of N_{\max} is divided into 100 intervals of equal length. Here n indicates the number of occurrence of single values of N_{\max} in each of such interval out of the total number of 3474.

of the mode function is reached. The deviations of isopycnal surfaces at other depths are described by the following equation:

$$\zeta(z, x, t) = \eta(x, t)\Phi(z) + \eta^2(x, t)F(z), \quad (5)$$

where $F(z)$ is the (first-order) nonlinear correction to the vertical mode function $\Phi(z)$. This correction is

evaluated from the following inhomogeneous boundary problem:

$$\frac{d^2 F}{dz^2} + \frac{N^2}{c^2} F = -\frac{\alpha}{c} \frac{d^2 \Phi}{dz^2} + \frac{3}{2} \frac{d}{dz} \left[\left(\frac{d\Phi}{dz} \right)^2 \right], \quad (6)$$

$$F(0) = F(H) = 0; \quad F(z_{\max}) = 0. \quad (7)$$

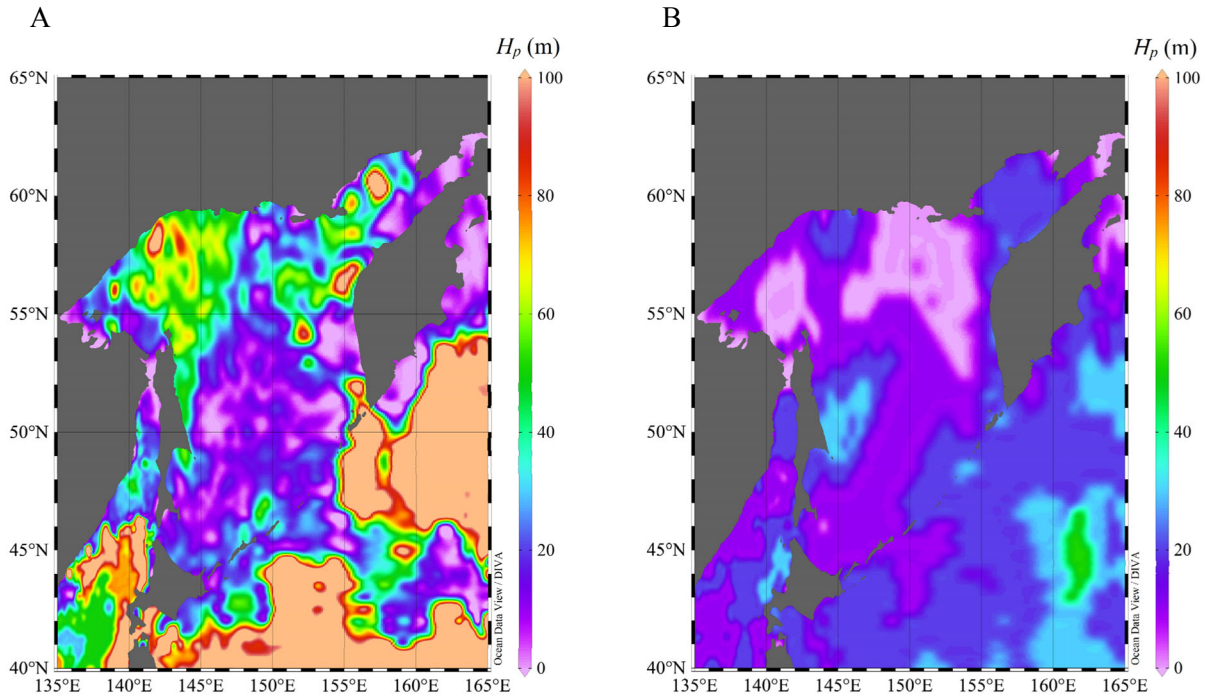


Fig. 4. Maps of the depths H_p (colour scale, m) where the Brunt–Väisälä frequency $N(z)$ reaches its maximum values in January (**A**) and July (**B**).

The coefficients α , α_1 and β are expressed using these functions as follows:

$$\alpha = \frac{3c}{2D} \int_0^H \left(\frac{d\Phi}{dz} \right)^3 dz, \quad D = \int_0^H \left(\frac{d\Phi}{dz} \right)^2 dz, \quad (8)$$

$$\beta = \frac{c}{2D} \int_0^H \Phi^2 dz, \quad (9)$$

$$\alpha_1 = \frac{1}{2D} \int_0^H dz \left\{ 9c \frac{dF}{dz} \left(\frac{d\Phi}{dz} \right)^2 - 6c \left(\frac{d\Phi}{dz} \right)^4 + 5\alpha \left(\frac{d\Phi}{dz} \right)^3 - 4\alpha \frac{dF}{dz} \frac{d\Phi}{dz} - \frac{\alpha^2}{c} \left(\frac{d\Phi}{dz} \right)^2 \right\}. \quad (10)$$

Equation (9) indicates that the coefficient β is always nonnegative. The coefficients α (Eq. 8) and α_1 (Eq. 10) at the quadratic and cubic nonlinear terms may be positive or negative and may also vanish. The values of parameters c , α , α_1 and β obviously depend on the properties of the vertical stratification and the water depth. Spatial variations in the stratification and different features of bathymetry may lead to substantial changes in the magnitude of all these coefficients and even to a swap of the sign of coefficients at the nonlinear terms of

Gardner’s equation. These changes may be associated with major modifications of the propagation of internal waves and even to radical reshaping of the dynamics of the wave field (Talipova et al. 2011; Kurkina et al. 2015). This feature stresses the importance of an adequate evaluation of possible parameter values and associated propagation regimes of internal waves in various basins. This paper provides such climatologically valid estimates for the entire Sea of Okhotsk.

Seasonal changes in so-called linear parameters of internal wave propagation – the phase speed c (Fig. 5) and the coefficient at the dispersive term β (Fig. 6) – are insignificant. Also, the major features of spatial distributions of these parameters do not show any substantial changes over different seasons. Their maximum values (about 2 m s^{-1} and $9 \times 10^5 \text{ s}^{-1}$, respectively) are found in the deep-water area of the Kuril trench.

Spatial variations in the values of both these parameters are mostly governed by the water depth (cf. Fig. 1 with Figs 5 and 6). Also, both these parameters can be adequately approximated as quadratic functions $y = p_1 h^2 + p_2 h + p_3$. It is convenient to use the normalized water depth $h = (H - H_0)/\delta$, $H_0 = 988.4 \text{ m}$, $\delta = 1035 \text{ m}$ for this procedure. The relevant approximations (with 95%-confidence interval indicated in the brackets) are given by the following expressions:

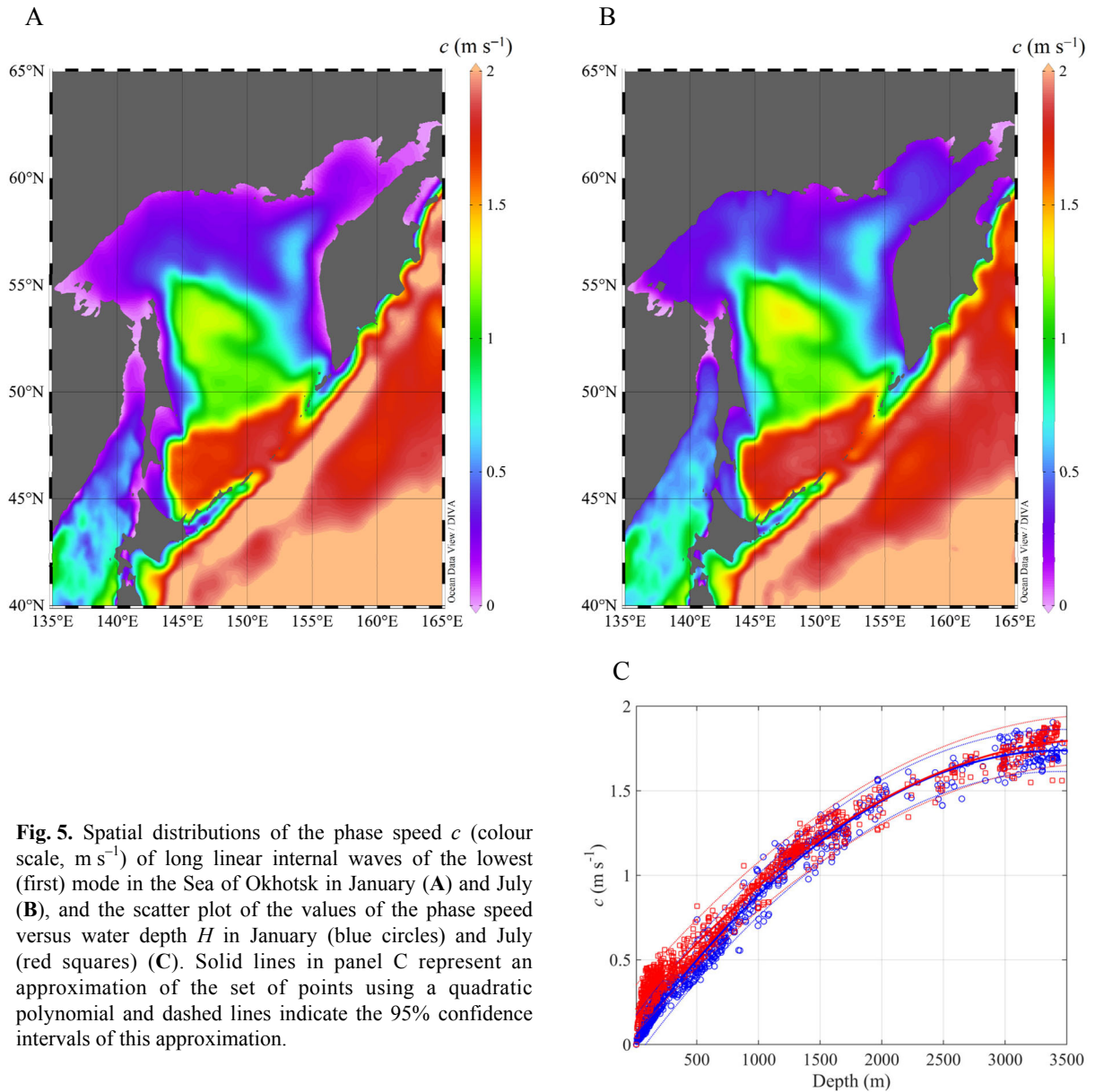


Fig. 5. Spatial distributions of the phase speed c (colour scale, m s^{-1}) of long linear internal waves of the lowest (first) mode in the Sea of Okhotsk in January (A) and July (B), and the scatter plot of the values of the phase speed versus water depth H in January (blue circles) and July (red squares) (C). Solid lines in panel C represent an approximation of the set of points using a quadratic polynomial and dashed lines indicate the 95% confidence intervals of this approximation.

– phase speed c , m s^{-1} , in January, $R^2 = 0.988$:

$$c = (-0.1527 \pm 0.0044) h^2 + (0.7263 \pm 0.0063) h + (0.8746 \pm 0.0058); \quad (11)$$

– phase speed c , m s^{-1} , in July, $R^2 = 0.981$:

$$c = (-0.1191 \pm 0.0051) h^2 + (0.6465 \pm 0.0073) h + (0.9275 \pm 0.0067); \quad (12)$$

– the coefficient β , $\text{m}^3 \text{s}^{-1}$, at the linear term in January and July, $R^2 = 0.996$:

$$\beta = (8.977 \pm 0.074) \times 10^4 h^2 + (1.32 \pm 0.01) h + (4.732 \pm 0.01). \quad (13)$$

As the values of the coefficient at the dispersive term β in January match well the similar values in July, the same approximation is eventually valid for the entire year.

The presented analysis reveals that the coefficients at the linear terms of Gardner's equation (phase speed c and the coefficient β at the dispersive term) exhibit only weak seasonal variations. Consequently, for first-order express estimates it is conditionally acceptable to use their annual average values. The largest seasonal variations in these parameters occur in relatively shallow shelf regions of the Sea of Okhotsk where it is still recommended to employ their seasonal values.

The coefficients at nonlinear terms α and α_1 (Figs 7, 8) are clearly more sensitive with respect to particular

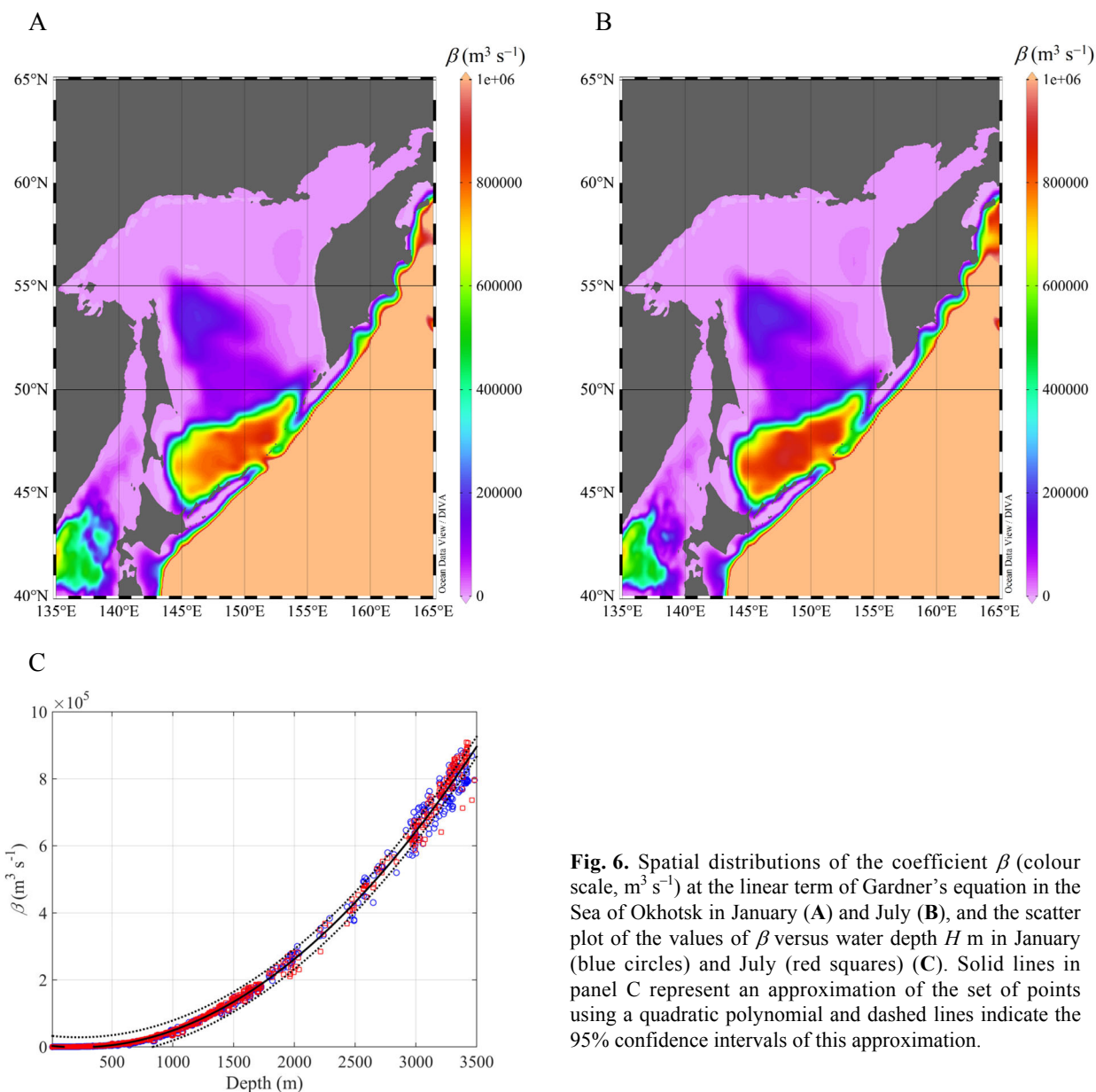


Fig. 6. Spatial distributions of the coefficient β (colour scale, $\text{m}^3 \text{s}^{-1}$) at the linear term of Gardner’s equation in the Sea of Okhotsk in January (A) and July (B), and the scatter plot of the values of β versus water depth H m in January (blue circles) and July (red squares) (C). Solid lines in panel C represent an approximation of the set of points using a quadratic polynomial and dashed lines indicate the 95% confidence intervals of this approximation.

seasonal structure of water masses. They exhibit substantial seasonal variations and in some regions even vanish or change their sign.

The values of the coefficient α at the quadratic term of Gardner’s equation lie in the interval of $(-0.01; 0.01) \text{ s}^{-1}$ in January (Fig. 8A). The magnitudes of negative examples of this coefficient are larger and extend to -0.03 in July (Fig. 8B). While most of the values of α are negative, there are several sea areas where this coefficient is positive in January. Such areas are found near the shores in the Strait of Sakhalin, in some small bays, in the northeastern shelf sea of Sakhalin, to the west of the Kamchatka Peninsula and in the central region of the Sea of Okhotsk. Such areas are only present

in winter. Most of them disappear in summer when the coefficient α becomes negative in the almost entire Sea of Okhotsk. The absolute values of α increase in shelf regions of the sea and its typical values reach -0.01 s^{-1} . The polarity of solitary internal waves generated at underwater slopes matches the sign of this coefficient. Consequently, solitary internal waves should predominantly have negative polarity in the Sea of Okhotsk. This conjecture matches the existing observational data (Nagovitsyn & Pelinovsky 1988; Nagovitsyn et al. 1991).

The coefficients α_1 at the cubic term of Gardner’s equation are generally very small in the entire sea in January. Relatively large positive values (up to $0.0002 \text{ m}^{-1} \text{ s}^{-1}$) occur only in a few elongated areas.

One such area stretches from the western shore of the Kamchatka Peninsula towards the eastern coast of Sakhalin. Somewhat smaller in magnitude but negative values are located on the northern shelf of the Sea of Okhotsk.

The distribution in question is greatly different in summer. There are extensive areas of comparatively large (up to $0.0002\text{--}0.0004\text{ m}^{-1}\text{ s}^{-1}$) positive values of α_1 whereas the domains with negative values of this coefficient shrink considerably. This distribution may substantially modify propagation properties of internal waves. In the areas of positive values of α_1 the phase speed c of long linear internal waves is about 0.3 m s^{-1} . The first-order nonlinear correction to this speed for waves with a reasonable amplitude of 10 m is about 0.1 m s^{-1} and thus on the order of $1/3$ of the linear wave speed. The impact of the cubic nonlinearity adds approximately 0.03 m s^{-1} , that is, another 10% of the linear wave speed. Consequently, wave dynamics may markedly change from that of the purely linear wave regime in areas where both α and α_1 are relatively large. As the particular values of the coefficients at the nonlinear terms of Gardner's equation are very sensitive with respect to small variations in the stratification of water masses, the presented estimates based on climatological maps of these parameters should be interpreted as indicative.

TRANSFORMATION OF THE BAROCLINIC INTERNAL TIDE INTO A SOLIBORE

To demonstrate some applications of the constructed maps of various coefficients of Gardner's equation, we consider the process of the formation of internal waves from the baroclinic internal tide in typical conditions of the northeastern shelf of Sakhalin and the adjacent continental slope in the winter (January) and summer (July) seasons. We use the Gardner model (Eqs (2)–(10)) as the basis of our estimates. This model is applied to a horizontally inhomogeneous case. The relevant modifications towards the use of spatially varying coefficients are described in detail in Talipova et al. (2014) and Kurkina et al. (2017a).

It is well known that a classic (barotropic) tide that propagates from the deep ocean into stratified water masses on the continental slope often transforms into a baroclinic tide (Vlasenko et al. 2005). We use this phenomenon as a boundary condition at the oceanside border of the combined shallow-water shelf region and continental slope of the sea and follow the further propagation of the internal wave along the transect indicated in Fig. 1. We assume that a baroclinic tidal wave with a sinusoidal shape

$$\eta(t, x = 0) = A \sin\left(\frac{2\pi}{T_{M2}}t\right),$$

amplitude of $A = 10\text{ m}$ and period of $T_{M2} = 12.4\text{ h}$ propagates from its likely generation area (the relatively steep slope from the nearshore of Sakhalin towards the central basin of the Sea of Okhotsk) towards the shores of Sakhalin. As the nearshore and the adjacent continental slope are almost homogeneous (that is, the bottom isolines are almost parallel to each other), it is acceptable to assume that the process generates a plane wave. This assumption greatly simplifies the modelling problem without any substantial loss of generality.

The starting point of the transformation of the baroclinic tide into an internal wave is chosen at a distance of 153 km from the shoreline in an area where the almost horizontal seabed of the central basin of the Sea of Okhotsk ends and the continental slope starts. This location is called the origin (of the transect) below. The typical values of the coefficients of Gardner's equation (2) all vary greatly along this transect in both seasons (Fig. 9). It is not unexpected that the (linear) propagation speed of such an internal wave is almost independent of the particular season. The difference between the typical values of the coefficient β at the dispersive term of Gardner's equation in January and July reaches up to 10% . Importantly, the coefficients α and α_1 at the nonlinear terms of this equation vary largely and in many occasions even their signs are different in summer and winter. Consistently with the above (Fig. 7), the coefficient α at the quadratic term is negative along the entire transect in January. It has relatively small magnitude in a part of the transect ($80\text{--}90\text{ km}$ from its origin), reaches its maximum absolute value $-2 \times 10^{-3}\text{ s}^{-1}$ at a distance of about 125 km from the origin and vanishes in the nearshore. The coefficient α turns into zero at a distance of 150 km from the origin. This happens in shallow water where the depth is only 130 m (Fig. 7A).

The values of the coefficient α_1 at the cubic term have predominantly a very small magnitude (of the order of 10^{-4}) during both seasons. The values of α_1 are particularly small in January. This parameter changes its sign at a distance of about $80\text{--}90\text{ km}$ from the origin; however, its magnitude remains small. The maximum of $|\alpha_1| \approx 6 \times 10^{-5}\text{ m}^{-1}\text{ s}^{-1}$ is located at the landward end of the transect. The results indicate that the shape of internal solitons is governed by the sign of the coefficient α at the quadratic term and thus internal solitons propagating along this transect have exclusively negative polarity in winter.

To characterize the changes in the wave amplitude owing to changes in the surrounding environment (water depth and stratification), we use an analogue

of the shoaling coefficient for surface waves in a linear approximation (Talipova et al. 2014). Changes in this parameter (Q in Fig. 9) signal that the amplitudes of internal solitons propagating along this transect increase considerably (by a factor of 1.5 in July and up to three times in January). It is thus likely that large-amplitude internal solitons are regularly present in the nearshore of northwestern Sakhalin. The discussed pattern of changes in the coefficient α_1 at the cubic term indicates that these solitons will transform into ‘fat’ or table-like disturbances. Such phenomena excite large vertical velocities and often drive strong mixing in affected areas.

The coefficient α at the quadratic term is negative everywhere in July. Its values change smoothly from very small ones in the deeper part of the transect up to the level of $-8 \times 10^{-3} \text{ s}^{-1}$ at the landward end of the transect. On the contrary, the coefficient α_1 at the cubic term is exclusively positive in July. Its values increase smoothly from almost zero in the deeper part of the transect up to about $4 \times 10^{-4} \text{ m}^{-1} \text{ s}^{-1}$ at the landward end. Consequently, internal solitons of both polarities may exist in this region in summer months. The maxima of the coefficient Q are much smaller in July than in January, therefore, the amplitudes of internal solitons at the landward end of the transect are apparently smaller in July than in January.

The described differences in the values of the coefficients of Gardner’s equation (2) obviously affect the properties of the propagation and transformations of several classes of solitary internal waves. To illustrate the possible extent of changes that a soliton may experience along the transect indicated in Fig. 1, we consider two scenarios of the formation of solibores (Figs 10, 11).

In typical conditions of January the onset of the formation of solitons from the baroclinic tidal wave with an amplitude of 10 m is located at a distance of approximately 130 km from the origin of the transect. The emerging solitary waves further transform into solibores that consist of a ‘fat’ (table-like) soliton and one or two soliton-like disturbances that lag behind the table-like feature. Further on, at a distance of 137 km (Fig. 12A) from the origin the lag is larger but the leading table-like soliton is still in contact with the solibore. The amplitude of the leading disturbance has greatly increased compared to the amplitude of the forcing internal tide. The most affected isopycnal surface (at a depth where the mode function has its maximum) moves down by almost 70 m. In other words, we observe the 3.5-fold amplification of the forcing wave whereas the resulting disturbance is unipolar.

In summer the same forcing (a sinusoidal baroclinic tide with an amplitude of 10 m) leads to a somewhat faster formation of solitons and also to a somewhat more accelerated course of the entire process. A soliton

becomes discernible at a distance of 125 km (water depth 240 m) from the origin of the transect (Fig. 11). The further development is much faster than in winter. The leading soliton with an amplitude of 35 m practically separates from the subsequent waves already after 7 km, at a distance of 132 km (water depth 170 m) from the origin (Fig. 12B).

The leading soliton grows rapidly. Its numerically simulated amplitude is already 50 m at the landward end (150 km from the origin) of the transect where the water depth is only 120 m. For this water depth and the projected amplitude the weakly nonlinear Gardner’s model, strictly speaking, becomes invalid. It is not clear what exactly will happen with such chains of solitary internal waves. Most likely the largest waves break at some distance from the shore and create very strong mixing and a multitude of smaller-amplitude internal (solitary) waves.

Our results suggest that substantial amplification of amplitudes of internal waves is an intrinsic feature of wave propagation in this region. It is expected that in certain seasons quite usual amplitudes (about 5 m) of the semidiurnal internal tide will drive complicated patterns of internal solitons in the nearshore of Sakhalin, with the amplitude of the leading soliton of up to 35 m. The polarity of such solitons is defined by the sign of the coefficient α at the quadratic term of Gardner’s equation at a location of their onset, that is, approximately 110 km from the origin. As this term is negative and the coefficient α_1 at the cubic term is very small, the emerging solitons will have also negative polarity. The above-discussed changes in the coefficient α_1 at the cubic term do not change the polarity. Therefore, only the amplitude and shape of emerging solitons will change.

DISCUSSION AND CONCLUSIONS

It is well known that the core properties of the stratification of the upper layer of the Sea of Okhotsk have, similarly to other water bodies on temperate latitudes, strong seasonal variability. Some of its features resemble those in much more sheltered and/or brackish regions. Differently from the open ocean, the main pycnocline is located relatively close to the sea surface in winter (normally at a depth of 30–50 m) and much deeper (at a depth of about 100 m) in summer. Summer warming gives rise to a seasonal pycnocline that is located at a depth of 10–30 m.

The maxima of the Brunt–Väisälä frequency also vary substantially, from 0.01 s^{-1} in winter to 0.04 s^{-1} in summer. These features give rise to major changes in the propagation regimes of large-amplitude internal waves in winter and summer. Such changes evidently

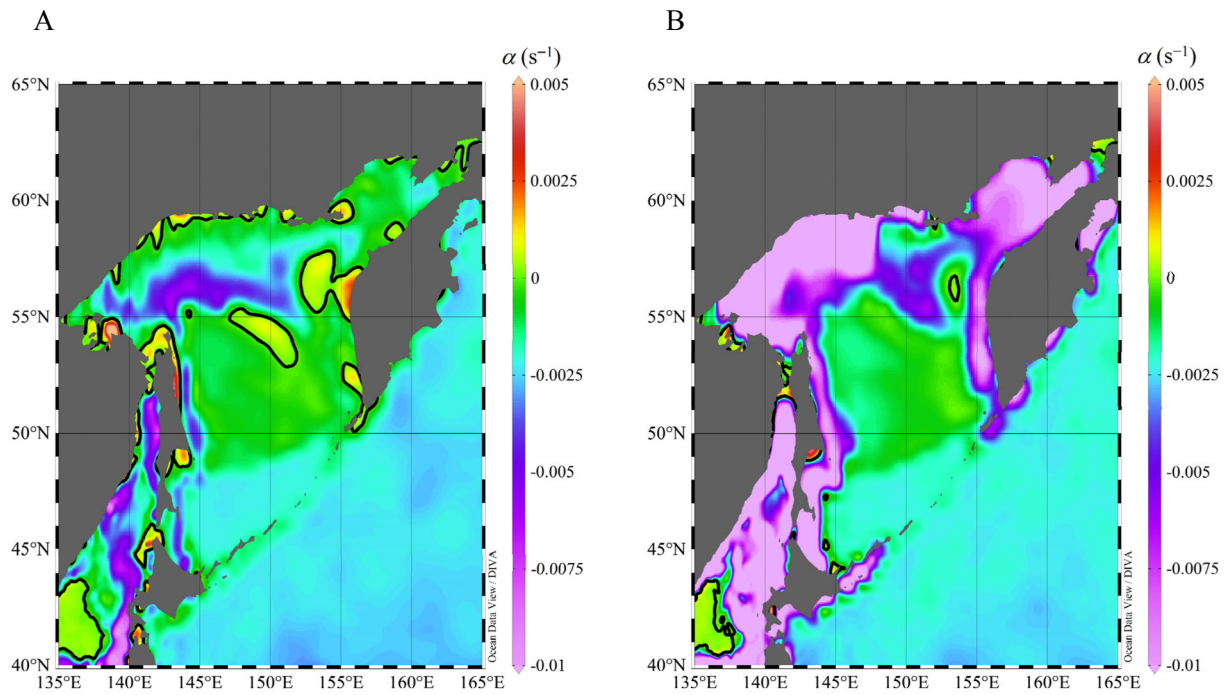


Fig. 7. Spatial distributions of the coefficient α (colour scale, s^{-1}) at the quadratic term of Gardner's equation in the Sea of Okhotsk in January (A) and July (B). The coefficient α vanishes along the bold lines.

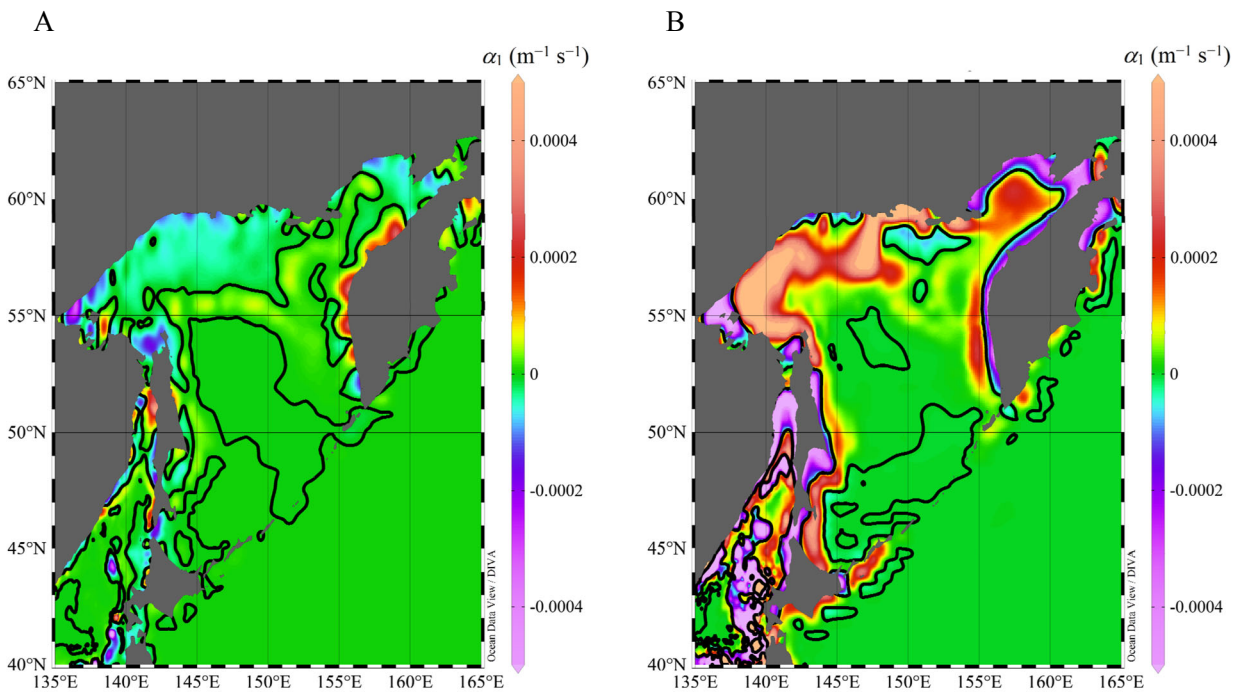


Fig. 8. Spatial distributions of the coefficient α_1 (colour scale, $\text{m}^{-1} \text{s}^{-1}$) at the cubic term of Gardner's equation in the Sea of Okhotsk in January (A) and July (B). The coefficient α_1 vanishes along the bold lines.

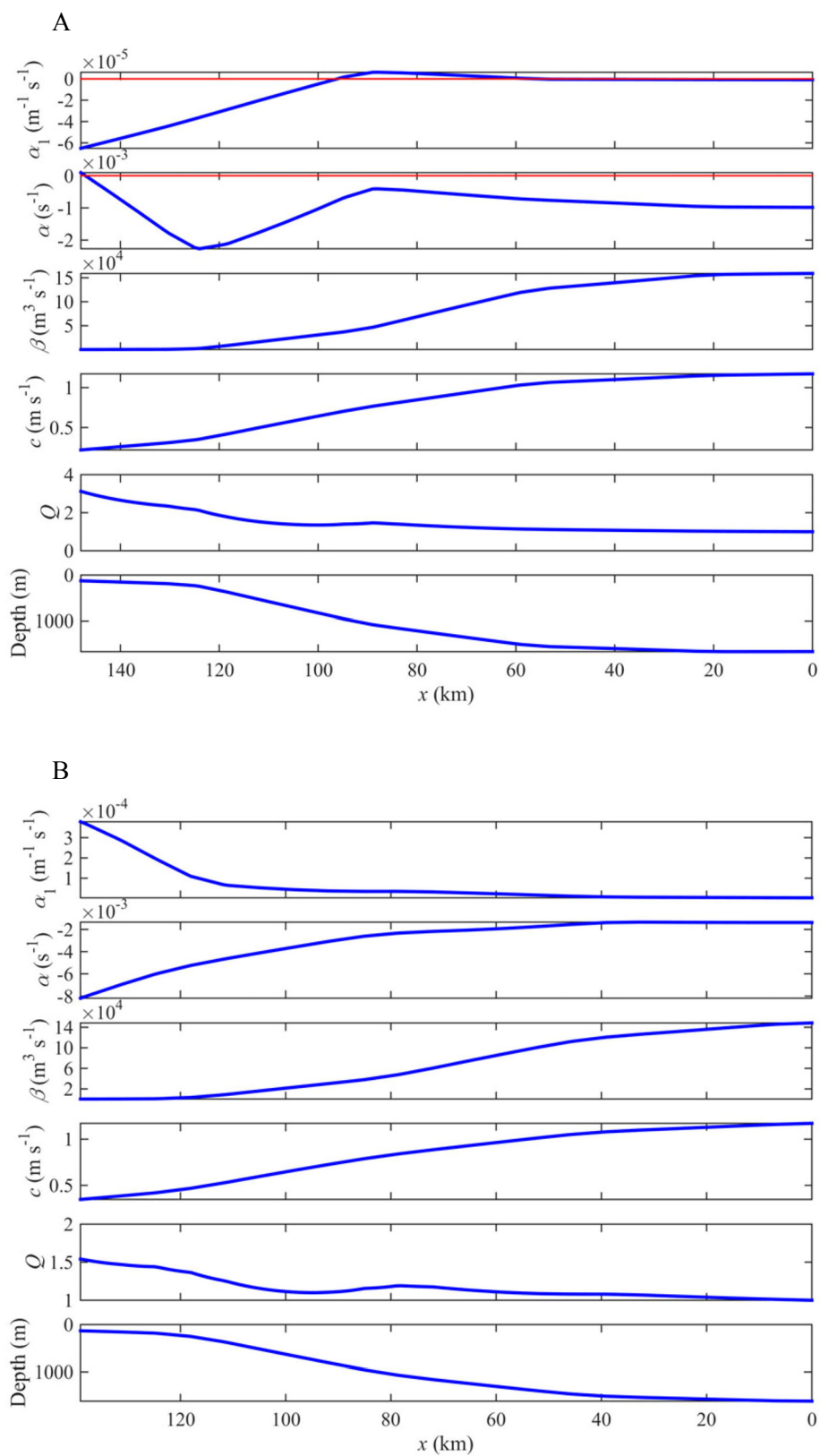


Fig. 9. Coefficients of Gardner's equation (2) along the transect on the continental shelf near the northeastern coast of Sakhalin in January (A) and July (B). The red line indicates the zero level.

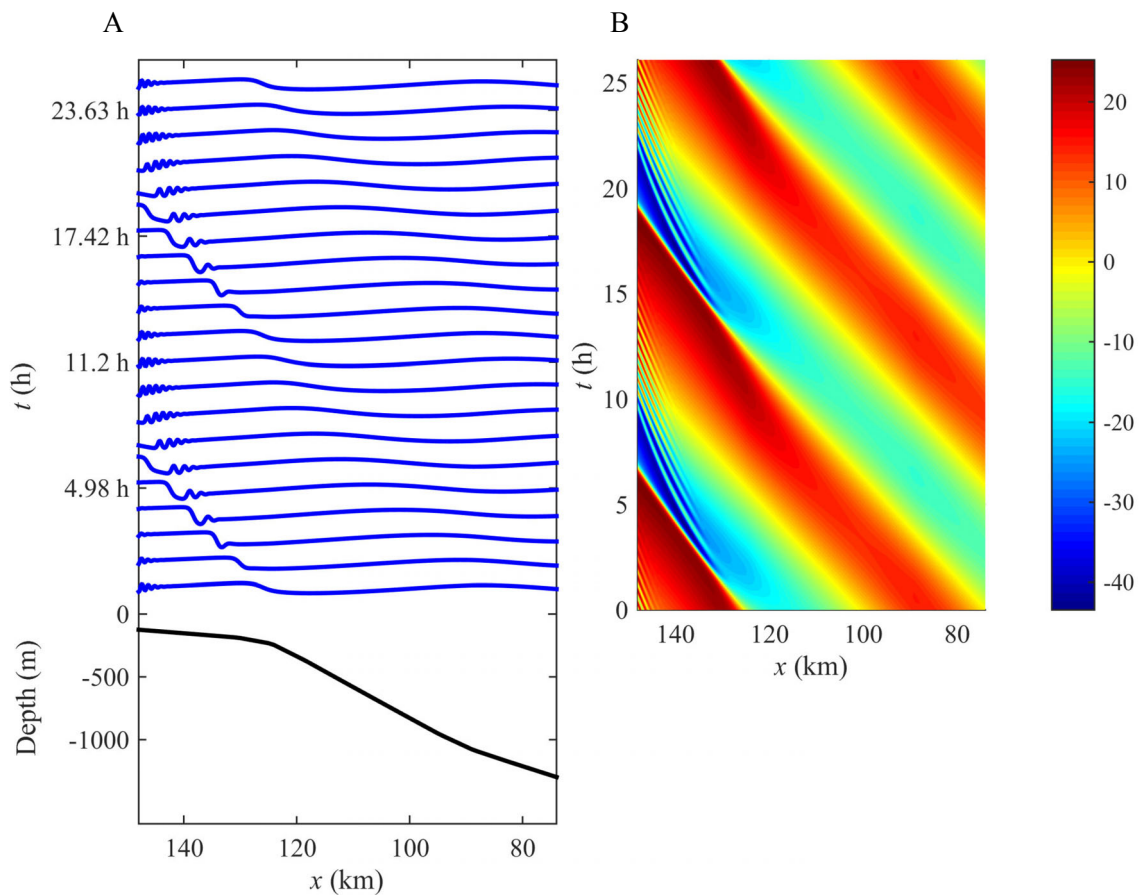


Fig. 10. Evolution of a baroclinic tide along the transect on the northeastern continental slope of Sakhalin (Fig. 1) in January: (A) deviations of isopycnal surfaces at different time instants along the transect. The solid line shows water depth and the distance is given from the deep-water end (origin) of the transect; (B) space–time (x – t) diagram of these surfaces (colour scale, m).

occur also in other water bodies with qualitatively similar stratification properties such as the Baltic Sea.

As expected, the propagation speed of long linear internal waves and dispersion properties of internal waves are largely invariant in the Sea of Okhotsk with respect to seasonal changes in stratification. The coefficients at the nonlinear terms of the governing (Gardner’s) equation are much more sensitive to seasons, being either negative or positive. Their largest absolute values are found in shallow nearshore areas.

Even though winter stratification is relatively weak and the typical values of the coefficient at the cubic nonlinearity of Gardner’s equation are of the order of $10^{-5} \text{ m}^{-1} \text{ s}^{-1}$, the effects driven by the presence of the cubic nonlinear term are decisive in some regions of the sea. This kind of impact is associated with the presence of areas where the coefficient at the quadratic term of Gardner’s equation vanishes. Such a situation is characteristic along transects on the shelf and continental slope of the eastern coast of Sakhalin where internal tide is the

main driving force of internal waves. Such a tide with a realistic amplitude of 10 m in wintertime conditions may create (after a chain of transformations on the continental slope) a prominent solibore that contains an up to 70 m high kink followed by a ‘fat’ (table-like) internal soliton. Similar effects are also pronounced in summer when the summer-type stratification may support the generation and propagation of Gardner solitons with an amplitude of up to 25–30 m.

The described essential difference in the amplification rates of internal solitons in January and July stems from the large difference in the variations in water density in summer and winter. The typical total variation in water density from the sea surface to the seabed is about 1 kg m^{-3} in winter but increases by almost a factor of two, up to almost 2 kg m^{-3} owing to warming and presence of less salty water in summer.

Our modelling exercises employ the classic weakly nonlinear models of internal waves. The relevant governing equations belong to the family of Korteweg–

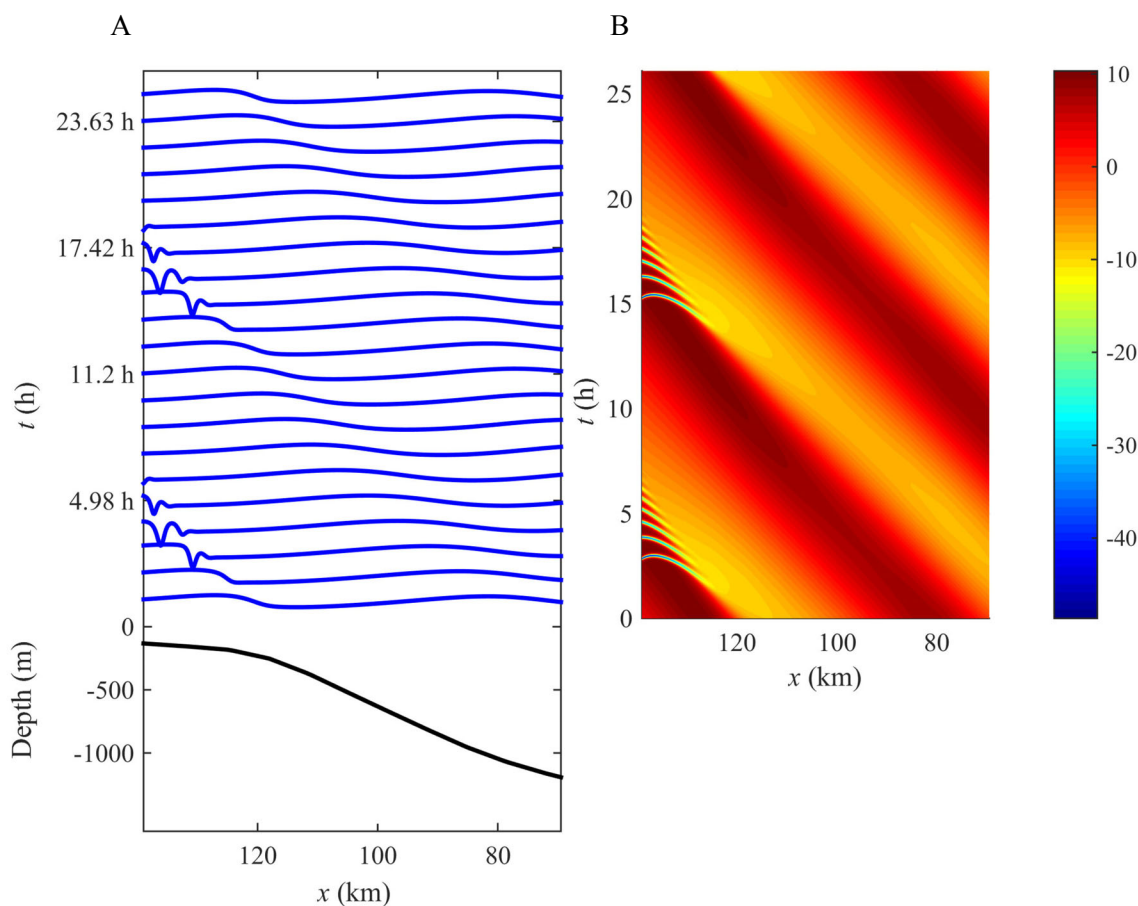


Fig. 11. Evolution of a baroclinic tide along the transect on the northeastern continental slope of Sakhalin (Fig. 1) in July. The notations are the same as for Fig. 10.

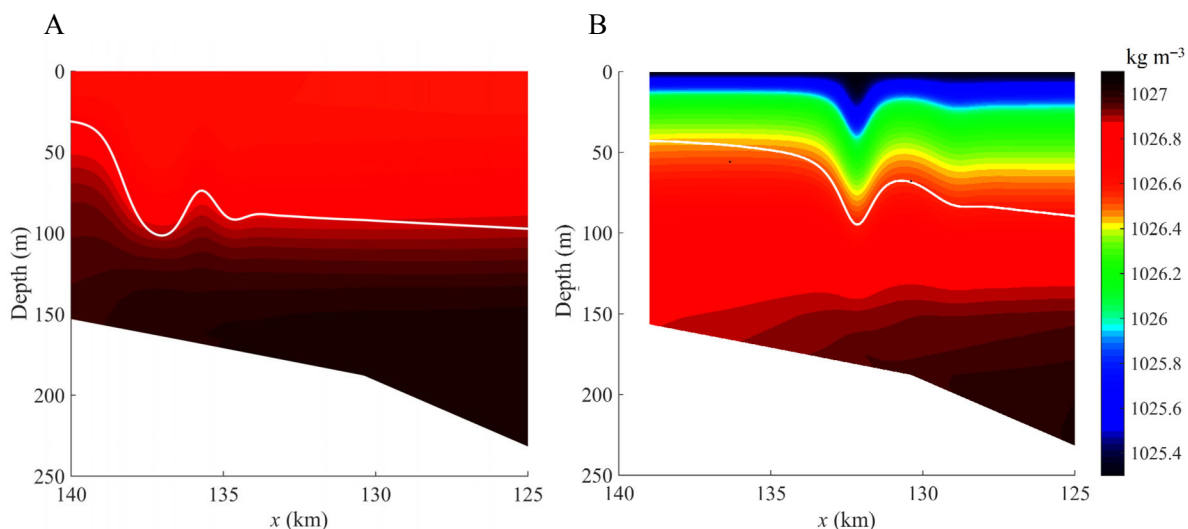


Fig. 12. Simulated deviations of isopycnal surfaces from their undisturbed position in the field of solibores driven by an internal tidal wave with an amplitude of 10 m along the transect indicated in Fig. 1 in January (A) and July (B). The distance is given from the deep-water end (origin) of the transect. The white line indicates deviations of the isopycnal surface at the location where the modal function reaches its maximum. This deviation is directly described by Gardner’s equation.

de Vries equations. These equations, including Gardner's equation (2), are, strictly speaking, only capable of replication of one-dimensional fields of motion in a spatially homogeneous field of density in an ocean of constant depth.

Their straightforward extensions are applicable to a spatially changing stratification and water depth, however, the changes may only occur in the wave propagation direction and the situation must be homogeneous along the wave crests. Therefore, our results are, for example, valid for cases when a wave runs across a continental slope with straight isobaths and a constant stratification along these isobaths. Such situations often occur in the ocean. In these occasions Gardner's equation and its counterparts can be used for extensive analysis of various phenomena in the water column and associated changes in hydrophysical fields.

For example, it is straightforward to calculate horizontal and vertical velocities of water parcels in complicated fields of internal waves (Kurkina et al. 2011). These velocities depend on the properties of waves and on the particular environmental conditions. For example, the internal waves presented in Fig. 12 excite maximum speeds of water parcels at the sea surface and at the seabed approximately 0.2 m s^{-1} in January and 0.3 m s^{-1} in July.

Acknowledgements. This study was initiated in the framework of the state task programme in the sphere of scientific activity of the Ministry of Education and Science of the Russian Federation (projects Nos 5.4568.2017/6.7 and 5.1246.2017/4.6) and financially supported by this programme, grants of the President of the Russian Federation (NSh-6637.2016.5), Russian Foundation for Basic Research (grant No. 16-05-00049) and the institutional support IUT33-3 from the Estonian Research Council. The referees E. Pelinovsky and Y. Stepanyants are thanked for their valuable remarks on the manuscript. The publication costs of this article were partially covered by the Estonian Academy of Sciences.

REFERENCES

- Alford, M. H., Peacock, T., MacKinnon, J. A., Nash, J. D., Buijsman, M. C., Centuroni, L. R., Chao, S.-Y., Chang, M.-H., Farmer, D. M., Fringer, O. B., Fu, K.-H., Gallacher, P. C., Graber, H. C., Helfrich, K. R., Jachec, S. M., Jackson, C. R., Klymak, J. M., Ko, D. S., Jan, S., Johnston, T. M. S., Legg, S., Lee, I.-H., Lien, R.-C., Mercier, M. J., Moum, J. N., Musgrave, R., Park, J.-H., Pickering, A. I., Pinkel, R., Rainville, L., Ramp, S. R., Rudnick, D. L., Sarkar, S., Scotti, A., Simmons, H. L., St Laurent, L. C., Venayagamoorthy, S. K., Wang, Y.-H., Wang, J., Yang, Y. J., Paluszkiwicz, T. & Tang, T.-Y. 2015. The formation and fate of internal waves in the South China Sea. *Nature*, **521**(7550), 65–69.
- Bourgault, D., Morsilli, M., Richards, C., Neumeier, U. & Kelley, D. E. 2014. Sediment resuspension and nepheloid layers induced by long internal solitary waves shoaling orthogonally on uniform slopes. *Continental Shelf Research*, **72**, 21–33.
- Carnes, M. R. 2009. *Description and Evaluation of GDEM-V3.0*. Naval Research Laboratory (NRL) Report NRL/MR/7330-09-9165, Naval Research Laboratory, 27 pp.
- Grimshaw, R., Pelinovsky, E., Talipova, T. & Kurkin, A. 2004. Simulation of the transformation of internal solitary waves on oceanic shelves. *Journal of Physical Oceanography*, **34**, 2774–2791.
- Grimshaw, R., Talipova, T., Pelinovsky, E. & Kurkina, O. 2010. Internal solitary waves: propagation, deformation and disintegration. *Nonlinear Processes in Geophysics*, **17**, 633–649.
- Fofonoff, N. & Millard, R. Jr. 1983. Algorithms for computation of fundamental properties of seawater. *UNESCO Technical Paper in Marine Science*, **44**, 15–25.
- Holloway, P., Pelinovsky, E., Talipova, T. & Barnes, B. 1997. A nonlinear model of internal tide transformation on the Australian North West shelf. *Journal of Physical Oceanography*, **27**, 871–896.
- Ivanov, V. A., Pelinovsky, E. N. & Talipova, T. G. 1993. Recurrence frequency of internal wave amplitudes in the Mediterranean. *Oceanology*, **33**, 147–150.
- Jackson, C. R. 2004. *An Atlas of Internal Solitary-like Waves and Their Properties*. Prepared for Office of Naval Research, Code 322 PO. Global Ocean Associates, 560 pp. http://internalwaveatlas.com/Atlas2_PDF/IWAtlas2_Pg357_SeaofoOkhotsk.pdf [accessed 10 June 2017].
- Kurkina, O. E. & Talipova, T. G. 2011. Huge internal waves in the vicinity of the Spitsbergen Island (Barents Sea). *Natural Hazards and Earth System Sciences*, **11**, 981–986.
- Kurkina, O., Talipova, T., Pelinovsky, E. & Soomere, T. 2011. Mapping the internal wave field in the Baltic Sea in the context of sediment transport in shallow water. *Journal of Coastal Research*, **SI 64**, 2042–2047.
- Kurkina, O. E., Kurkin, A. A., Rouvinskaya, E. A. & Soomere, T. 2015. Propagation regimes of interfacial solitary waves in a three-layer fluid. *Nonlinear Processes in Geophysics*, **22**, 117–132.
- Kurkina, O. E., Kurkin, A. A., Pelinovsky, E. N., Semin, S. V., Talipova, T. G. & Churaev, E. N. 2016. Structure of currents in the soliton of an internal wave. *Oceanology*, **56**, 767–773.
- Kurkina, O., Rouvinskaya, E., Talipova, T. & Soomere, T. 2017a. Propagation regimes and populations of internal waves in the Mediterranean Sea basin. *Estuarine, Coastal and Shelf Science*, **185**, 44–54.
- Kurkina, O., Talipova, T., Soomere, T., Giniyatullin, A. & Kurkin, A. 2017b. Kinematic parameters of internal waves of the second mode in the South China Sea. *Nonlinear Processes in Geophysics*, **24**, 645–660.
- Lamb, K. & Yan, L. 1996. The evolution of long wave undular bores: comparisons of fully nonlinear numerical model with weakly nonlinear theory. *Journal of Physical Oceanography*, **26**, 2712–2734.
- Liao, G., Hua, X. X., Liang, C., Dong, C., Zhou, B., Ding, T., Huang, W. & Xu, D. 2014. Analysis of kinematic

- parameters of internal solitary waves in the northern South China Sea. *Deep-Sea Research*, **1**, **94**, 159–172.
- Liu, A. K., Su, F.-Ch., Hsu, M.-K., Kuo, N.-J. & Ho, Ch.-R. 2013. Generation and evolution of mode-two internal waves in the South China Sea. *Continental Shelf Research*, **59**, 18–27.
- Maderich, V., Talipova, T., Grimshaw, R., Pelinovsky, E., Choi, B. H., Brovchenko, I., Terletska, K. & Kim, D. C. 2009. Internal solitary wave transformation at the bottom step in two-layer flow: the Gardner and Navier–Stokes frameworks. *Nonlinear Processes in Geophysics*, **16**, 33–42.
- Maderich, V., Talipova, T., Grimshaw, R., Pelinovsky, E., Choi, B. H., Brovchenko, I. & Terletska, K. 2010. Interaction of a large amplitude interfacial solitary wave of depression with a bottom step. *Physics of Fluids*, **22**, Art. No. 076602.
- Nagovitsyn, A. P. & Pelinovsky, E. N. 1988. Observations of solitons of internal waves in the coastal zone of the Sea of Okhotsk. *Meteorology and Hydrology*, **4**, 124–126 [in Russian].
- Nagovitsyn, A. P., Pelinovsky, E. N. & Stepanyants, Yu. A. 1991. Observation and analysis of solitary internal waves in the coastal zone of the Sea of Okhotsk. *Soviet Journal of Physical Oceanography*, **2**, 65–70.
- Osborne, A. R. 2010. *Nonlinear Ocean Waves and the Inverse Scattering Transform*. Elsevier, San Diego, 944 pp.
- Pan, X., Wong, G. T. F., Shiah, F.-K. & Ho, T.-Y. 2012. Enhancement of biological productivity by internal waves: observations in the summertime in the northern South China Sea. *Journal of Oceanography*, **68**, 427–437.
- Pelinovsky, E., Polukhina, O., Slunyaev, A. & Talipova, T. 2007. Internal solitary waves. In *Solitary Waves in Fluids* (Grimshaw, R. H. J., ed.), pp. 85–110. WIT Press, Southampton, Boston.
- Pettersen, T. 2011. Largest accident in Russian oil sector. *Barents Observer*, December 22, 2011.
- Poloukhin, N. V., Talipova, T. G., Pelinovsky, E. N. & Lavrenov, I. V. 2003. Kinematic characteristics of the high-frequency internal wave field in the Arctic Ocean. *Oceanology*, **43**, 333–343.
- Polukhin, N. V., Pelinovsky, E. N., Talipova, T. G. & Muyakshin, S. I. 2004. On the effect of shear currents on the vertical structure and kinematic parameters of internal waves. *Oceanology*, **44**, 22–29.
- Ramp, S. R., Yang, Y. J. & Bahr, F. L. 2010. Characterizing the nonlinear internal wave climate in the northeastern South China Sea. *Nonlinear Processes in Geophysics*, **17**, 481–498.
- Reeder, D. B., Ma, B. B. & Yang, Y. J. 2011. Very large subaqueous sand dunes on the upper continental slope in the South China Sea generated by episodic, shoaling deep-water internal solitary waves. *Marine Geology*, **279**, 12–18.
- Rutenko, A. N. 2010. The influence of internal waves on losses during sound propagation on a shelf. *Acoustical Physics*, **56**, 703–713.
- Si, Z., Zhang, Y. & Fan, Z. 2012. A numerical simulation of shear forces and torques exerted by large-amplitude internal solitary waves on a rigid pile in South China Sea. *Applied Ocean Research*, **37**, 127–132.
- Song, Z. J., Teng, B., Gou, Y., Lua, L., Shi, Z. M., Xiao, Y. & Qu, Y. 2011. Comparisons of internal solitary wave and surface wave actions on marine structures and their responses. *Applied Ocean Research*, **33**, 120–129.
- Stastna, M. & Lamb, K. G. 2008. Sediment resuspension mechanisms associated with internal waves in coastal waters. *Journal of Geophysical Research*, **113**, Art. No. C10016.
- Stober, U. & Moum, J. N. 2011. On the potential for automated realtime detection of nonlinear internal waves from seafloor pressure measurements. *Applied Ocean Research*, **33**, 275–285.
- Talipova, T. G. & Pelinovsky, E. N. 2013. Modeling of propagating long internal waves in an inhomogeneous ocean: the theory and its verification. *Fundamental and Applied Hydrophysics*, **6**, 46–54 [in Russian].
- Talipova, T., Pelinovsky, E. & Kõuts, T. 1998. Kinematics characteristics of the internal wave field in the Gotland Deep in the Baltic Sea. *Oceanology*, **38**, 33–42.
- Talipova, T. G., Pelinovsky, E. N. & Kharif, Ch. 2011. Modulational instability of long internal waves of moderate amplitudes in a stratified and horizontally inhomogeneous ocean. *JETP Letters*, **94**, 182–186.
- Talipova, T. G., Pelinovsky, E. N., Kurkin, A. A. & Kurkina, O. E. 2014. Modeling the dynamics of intense internal waves on the shelf. *Izvestiya, Atmospheric and Oceanic Physics*, **50**, 630–637.
- Talipova, T. G., Kurkina, O. E., Rouvinskaya, E. A. & Pelinovsky, E. N. 2015. Propagation of solitary internal waves in two-layer ocean of variable depth. *Izvestiya, Atmospheric and Oceanic Physics*, **51**, 89–97.
- Teague, W. J., Carron, M. J. & Hogan, P. J. 1990. A comparison between the Generalized Digital Environmental Model and Levitus climatologies. *Journal of Geophysical Research*, **95**, 7167–7183.
- Vázquez, A., Flecha, S., Bruno, M., Macías, D. & Navarro, G. 2009. Internal waves and short-scale distribution patterns of chlorophyll in the Strait of Gibraltar and Alborán Sea. *Geophysical Research Letters*, **36**, Art. No. L23601.
- Vlasenko, V. & Stashchuk, N. 2015. Internal tides near the Celtic sea shelf break: a new look at a well known problem. *Deep Sea Research*, **1**, **103**, 24–36.
- Vlasenko, V., Stashchuk, N. & Hutter, K. 2005. *Baroclinic Tides: Theoretical Modeling and Observational Evidence*. Cambridge University Press, Cambridge, 348 pp.
- Xu, J., Chen, Z., Xie, J. & Cai, S. 2016. On generation and evolution of seaward propagating internal solitary waves in the northwestern South China Sea. *Communications in Nonlinear Science and Numerical Simulation*, **32**, 122–136.
- Zonn, I. S. & Kostianoy, A. G. 2009. *Okhotskoe More [Sea of Okhotsk]*. Encyclopedia. Publishing house “International relations”, Moscow, 256 pp. [in Russian].
- Warn-Varnas, A., Chin-Bing, S. A., King, D. B., Hawkins, J. & Lamb, K. 2009. Effects on acoustics caused by ocean solitons, Part A. *Oceanography. Nonlinear Analysis*, **71**, e1807–e1817.

Veemasside stratifikatsiooni sesoonsete muutuste mõju siselainete dünaamikale Ohhoota meres

Oxana E. Kurkina, Tatyana G. Talipova, Tarmo Soomere, Andrey A. Kurkin ja Artem V. Rybin

Siselainete omadused ja dünaamika sõltuvad oluliselt veemasside vertikaalsest struktuurist ehk stratifikatsioonist. Sarnaselt Läänemerele varieeruvad ka Ohhoota meres stratifikatsiooni omadused tugevasti nii erinevates mere osades kui ka aastaegade lõikes. On analüüsitud, kuidas taolised muutused mõjutavad nõrgalt mittelineaarsete siselainete omadusi ja käitumist kirjeldava Gardneri võrrandi parameetrite väärtusi, ning konstrueeritud selliste lainete faasikiiruse ja kõnesoleva võrrandi kõigi liikmete kordajate väärtuste kaardid erinevate aastaegade jaoks. Saadud kaardid võimaldavad kiiresti hinnata siselainete (sh solitonide) peamisi omadusi ja valida sobiv parameetrite komplekt selliste lainete reprodutseerimiseks arvutusmudelites. On näidatud, et pikkade nõrgalt mittelineaarsete siselainete faasikiirus aastaegade lõikes praktiliselt ei muutu. Gardneri võrrandi ruutliikme kordaja on suuremas osas merest negatiivne nii suvel kui ka talvel; seega on solitonilaadsed siselained selles meres harilikult negatiivse polaarsusega (st püknokliin liigub laines sügavamale). Numbriliste eksperimentide abil on näidatud, et Gardneri võrrandi kuupliikme kordaja väärtuste tuntava muutumisega eri aastaegadel kaasnevad üldjuhul solitonide ja nende ahelate kujus olulised muutused.